



Cite this: *J. Mater. Chem. B*,  
2024, 12, 991

## The effect of oxygen supply using perfluorocarbon-based nanoemulsions on human hair growth†

Phil June Park, <sup>a</sup> Himangsu Mondal, <sup>b</sup> Bong Soo Pi, <sup>ad</sup> Sung Tae Kim <sup>c</sup> and Jun-Pil Jee <sup>b</sup>

Hair dermal papilla cells (hDPCs) play a crucial role in hair growth and regeneration, and their function is influenced by nutrient and oxygen supply. A microenvironment with significantly low oxygen ( $O_2$ ) levels, known as anoxic conditions ( $<0.2\%$ ) due to oxygen deficiency, hinders hDPC promotion and retards hair regrowth. Here, a nanoemulsion (NE) based on perfluoroctyl bromide (PFOB), a member of the perfluorocarbon family, is presented to provide a sustainable  $O_2$  supply and maintain physical stability *in vitro*. The PFOB-NE has been shown to continuously release oxygen for 36 h, increasing and maintaining the  $O_2$  concentration in the anoxic microenvironment of up to 0.8%. This sustainable  $O_2$  supply using PFOB-NE has promoted hDPC growth and also induced a complex cascade of effects. These effects encompass regulation via inhibiting lactate accumulation caused via oxygen deficiency, increasing lactate dehydrogenase activity, and promoting the expression of genes, such as the hypoxia-inducible factor 1 family and NADPH oxidase 4 under anoxic conditions. Sustained  $O_2$  supply is shown to enhance human hair organ elongation approximately four times compared to the control under anoxic conditions. In conclusion, the perfluorocarbon-based NE containing oxygen proves to be an important strategic tool for improving hair growth and alleviating hair loss.

Received 25th September 2023,  
Accepted 7th December 2023

DOI: 10.1039/d3tb02237d

rsc.li/materials-b

## 1. Introduction

Hair loss is a phenomenon more complex than the process of hair falling off the scalp *via* hair follicle miniaturization, involving various internal and external physiological factors.<sup>1–3</sup> The major systemic causes of hair loss include telogen effluvium, nutrition, endocrine imbalances, drugs, infections, diseases, and malignancy.<sup>4–7</sup> Hair loss alone is not life-threatening; it is distressing and causes a loss of self-esteem, increased depressive feelings, and has socially negative effects on an individual.<sup>8</sup> Hence, the alleviation of hair loss or stimulation of hair regrowth in patients with hair loss must be determined.

The main function of the blood vessels is to supply various nutrients and oxygen ( $O_2$ ) to all body organs and tissues.<sup>9,10</sup> A sufficient supply of nutrients has been previously reported

to play an important role in hair growth.<sup>11,12</sup> These nutrients include fatty acids (e.g., linoleic acid and  $\alpha$ -linoleic acid), proteins, vitamins (e.g., vitamin A), and metallic cofactors (e.g., Zn, Fe, and Se).<sup>13–15</sup> Moreover,  $O_2$  supply can be a critical factor because the nutrients and  $O_2$  provision of the blood vessels in the dermal papillae nourish the hair follicles.<sup>16–18</sup>  $O_2$  is an essential element for cell survival<sup>19</sup> and plays an important role in hair growth and cycling.<sup>17,20</sup> A moderate supply of  $O_2$  maintains a healthy scalp and encourages hair growth.<sup>21,22</sup> A previous study revealed that hair dermal papilla cells (DPCs), which are key cells in hair follicle cycling, are affected by  $O_2$  concentration and consequently, the related lactate dehydrogenase activity.<sup>23,24</sup> Furthermore, hair growth is closely associated with vascularization and angiogenesis.<sup>25</sup> In particular, the vascular endothelial growth factor (VEGF) is closely associated with hair growth; minoxidil facilitates the upregulation of VEGF levels in human DPCs (hDPCs) and is widely used in hair loss treatment.<sup>26,27</sup> These therapeutic agents provide a nurturing environment for hair dermal papillae *via* vascular smooth muscle relaxation and improvement in the blood supply for hair growth; however, their mode of action remains to be completely elucidated.  $O_2$  transporting agents represent another factor of consideration for optimal hair growth.

Perfluorocarbons (PFCs), composed of fluorine and carbon, are organofluorine compounds that are useful as  $O_2$ -carrying

<sup>a</sup> Basic Research & Innovation Division, AMOREPACIFIC R&I Center, Gyeonggi-do, 17074, Republic of Korea

<sup>b</sup> College of Pharmacy, Chosun University, Gwangju, 61452, Republic of Korea

<sup>c</sup> Department of Pharmaceutical Engineering/Department of Nanoscience and Engineering, Inje University, Gyeongsangnam-do, 50834, Republic of Korea

<sup>d</sup> Department of Chemical and Biomolecular Engineering, Korea Advanced Institute of Science and Technology (KAIST), Daejeon 34141, Republic of Korea

† Electronic supplementary information (ESI) available. See DOI: <https://doi.org/10.1039/d3tb02237d>

‡ These authors contributed equally to this work.



agents.<sup>28,29</sup> Oxygent (Alliance Pharmaceutical Corp.), composed of perfluoroctyl bromide (PFOB) and perfluorodecyl bromide, has been developed as an artificial red blood cell that intravascularly delivers O<sub>2</sub> to the human body.<sup>30</sup> PFCs can dissolve considerable quantities of O<sub>2</sub>, and the most common PFCs used are perfluoroctyl bromide (C<sub>8</sub>BrF<sub>17</sub>), perfluorodecalin (PFD, C<sub>10</sub>F<sub>18</sub>), PFOB (527 mL O<sub>2</sub> L<sup>-1</sup> PFC), and PFD (403 mL O<sub>2</sub> L<sup>-1</sup> PFC) at 1 atm and 25 °C, respectively. PFCs exhibit a high capacity for O<sub>2</sub> compared to that of water (9–10 mL O<sub>2</sub> L<sup>-1</sup> water) and blood (200 mL O<sub>2</sub> L<sup>-1</sup> blood).<sup>31</sup> In addition, most PFCs are chemically inactive, nontoxic, noninflammable, and have a variety of cellular applications.<sup>32</sup> Despite their high O<sub>2</sub> capacity and biocompatibility, the use of PFCs is limited for biological and clinical applications because they are immiscible in water,<sup>33</sup> and require a safe and stable formulation for application. Thus, the aim of this study was to develop a suitable PFC formulation for O<sub>2</sub> transport.

The primary objective of this study was to fabricate optimized forms of PFOB nanoemulsions (PFOB-NEs) for O<sub>2</sub> delivery, utilizing co-surfactants such as Tween 80 and Lipoid 100. The second objective was to investigate the effects of exogenous O<sub>2</sub> supply on the growth and proliferation of hDPC cells, and to determine its positive impact on hair follicle organ culture derived from human sources, that ultimately promoted hair regrowth. The selected combinations for NE formulation were chosen due to their ability to provide high dissolved O<sub>2</sub> capacity, sustained release, and colloidal stability. Finally, we propose a strategic delivery of oxygen-loaded NEs through the skin as a means of targeted supply to hair follicles.

## 2. Materials and methods

### 2.1. Human hair follicles and cell culture

Non-balding scalp specimens were obtained from patients undergoing hair transplantation surgery. All experimental methods were approved by the medical ethics committee of Dankook Medical College (Cheonan, Republic of Korea), and informed written consent was obtained from all the patients (Institutional Review Board (IRB): DKUH 2020-11-004). Anagen human hair follicles were isolated from occipital scalp specimens obtained during the remaining hair transplantation surgeries. Human hair follicles were cultured in William's E medium (Sigma-Aldrich, USA) supplemented with 2 mM l-glutamine (Sigma Aldrich), 10 µg mL<sup>-1</sup> insulin (Sigma Aldrich), 10 ng mL<sup>-1</sup> hydrocortisone (Sigma Aldrich), 0.1% of fungizone (Gibco, USA), and 1% of antibiotic-antimycotic (Gibco).

The hDPCs were isolated from hair follicles and cultured in Dulbecco's modified Eagle's medium (Hyclone Laboratories, USA) supplemented with 10% fetal bovine serum (Gibco) and 1% of antibiotic-antimycotic and incubated at 37 °C in a 5% carbon dioxide incubator.

### 2.2. Preparation of PFOB-NE and filling-up O<sub>2</sub>

Lipoid S100 was donated by Lipoid GmbH (Ludwigshafen, Germany), polyoxyethylene sorbitan monooleate (Tween80) was purchased from Duksan Pure Chemicals (Gyeonggi-do,

Republic of Korea), and 1-bromoperfluorooctane was purchased from Synquest Laboratories (Florida, USA). Using these compounds, NEs were fabricated *via* the method described in our previous study.<sup>34</sup> In brief, 0.1875 g of Lipoid S 100, 0.0625 g of Tween 80, and 4.75 g of distilled water were transferred to a 20 mL glass vial. The vial was placed on a magnetic stirrer and stirred at 800 rpm at 37 °C for 12 h to obtain a uniform mixture, after which 5 g of PFOB was added and the mixture was homogenized for 30 s at 30 000 rpm using a high-speed homogenizer (Daihan Scientific, Gyeonggi-do, Republic of Korea) to form a crude emulsion. The crude emulsion was subsequently micro-fluidized using a Microfluidics-LV1 (Microfluidics, Massachusetts, USA) at high pressure (1500 psi) for five cycles; a fine emulsion was formed with a uniform texture and color. Prior to each experiment, O<sub>2</sub> gas purging was performed for 30 s to encapsulate O<sub>2</sub>.

### 2.3. Measurement of particle diameter and zeta potential

NEs were diluted 10-fold in double-distilled water to evaluate the particle diameters and zeta potentials, which were measured using a particle size analyzer ELSZ-2000 (Otsuka Electronics, Osaka, Japan).

### 2.4. TEM imaging

To obtain negatively stained TEM images, 5 µL of each sample (purified) was applied to carbon-coated grids that had been glow-discharged (Harrick Plasma, USA) for 1 min in air. The grids were negatively stained with 1% uranyl acetate. The prepared grids were observed using a Tecnai 10 transmission electron microscope (FEI, Instrumentation was used in the Kangwon Center for Systems Imaging) equipped with a lanthanum hexaboride (LaB<sub>6</sub>, FEI) cathode operating at 100 kV. The images were recorded using a 2 K × 2 K UltraScan CCD camera (Gatan, CA, USA). The instruments were installed at Kangwon Center for Systems Imaging, Chuncheon, Republic of Korea.

### 2.5. O<sub>2</sub> encapsulation and release evaluation

Each concentration of O<sub>2</sub> was monitored using a Neofox optical O<sub>2</sub> sensor (Ocean Optics, FL, USA), which quantitatively measures O<sub>2</sub> using optical fluorescence. O<sub>2</sub> purging was performed for 30 s to saturate and encapsulate O<sub>2</sub> into the NEs. O<sub>2</sub> release was monitored in an incubator at 37 °C. The concentration of O<sub>2</sub> in each sample was measured every 2 h. Each experiment was performed in triplicate and all samples were of the same volume.

### 2.6. Cell viability assay

The viability of the hDPCs after PFOB-NE treatment with or without O<sub>2</sub> was measured using the EZ-Cytotoxicity assay kit (Daeil Lab Service, Seoul, Republic of Korea) according to the manufacturer's instructions. Briefly, hDPCs were pre-cultured for 48 h in a 96-well plate and treated with various concentrations of PFOB-NE in the growth medium for 24 and 72 h, respectively. EZ-Cytotoxic solution (10 µL) was added to each well, following incubation at 37 °C for 2 h, and the absorbance was measured at 450 nm using a spectrophotometer (Synergy H2; BioTek, VT, USA). Each experiment



was performed in triplicate and data are presented as absorbance values.

## 2.7. Measurement of O<sub>2</sub> concentration in liquid media

A FireSting<sup>®</sup>-GO2 Pocket O<sub>2</sub> Meter (PyroScience GmbH, Dresden, Germany) was used to monitor O<sub>2</sub> in the liquid medium under normoxic, hypoxic, or anoxic conditions. To measure the continual changes in the O<sub>2</sub> concentration, the unit of the device was first set to percentage and the temperature and O<sub>2</sub> concentration probe were brought into close contact with the culture medium. Continual measurements were performed for 48 h at 2 h intervals. Each experiment was independently repeated thrice.

## 2.8. Lactate quantification

Lactate secretion was quantitatively analyzed using a lactate assay kit (Abcam, Cambridge, UK) according to the manufacturer's protocol. For the measurement of the lactate secretion, hDPCs at passage 3 were first plated at a density of  $2 \times 10^5$  cells per well in a six-well plate and incubated for 24 h. hDPCs were co-cultured with non-Oxy-NE or Oxy-NE for 36 h under conditions of normoxia, hypoxia and anoxia, respectively. The hDPCs were harvested using accutase solution (Millipore, MA, USA) and washed with cold phosphate-buffered saline (Corning Life Science, NY, USA). To obtain a clear solution, the remaining lactate enzyme was removed using a deproteinizing sample preparation kit (Abcam, Cambridge, UK) according to the manufacturer's protocol; the optical density was measured using an enzyme-linked immunosorbent assay (ELISA) reader (SPECTROstar Nano, BMG Labtech, Ortenberg, Germany) at 450 nm and relatively calculated according to the standard curve using L(+)-lactate.

## 2.9. Lactate dehydrogenase activity

Lactate dehydrogenase was measured using an LDH assay kit (Abcam, Cambridge, UK) according to the manufacturer's protocol. For the measurement of the LDH activity, hDPCs were cultured vigorously under the same protocol as that used in the previous lactate quantification experiment. Thereafter, each optical density was measured using an ELISA reader at 450 nm and calculated according to the standard curve using NADH.

## 2.10. RNA extraction and RT-qPCR

A ReliaPrep<sup>™</sup> RNA Cell Miniprep System (Promega, WI, USA) was used for total RNA extraction from the hDPCs according to the manufacturer's instructions. The RevertAid First Strand cDNA Synthesis Kit (Thermo Fisher Scientific, MA, USA) was used to synthesize cDNA. The synthesized cDNA was used as a template for gene expression analysis using a 7500 Fast Real-Time PCR System (Life Technologies, MA, USA) with the following TaqMan probes: HIF1 $\alpha$  (Hs00153153\_m1), HIF1 $\beta$  (Hs01121918\_m1),  $\beta$ -catenin (Hs0355045\_m1), APC (Hs01568269\_m1), TCF4 (Hs00162613\_m1), NOX4 (Hs01379108\_m), LDHA (Hs01378790\_g1), LDHB (Hs00929956\_m1), and glyceraldehyde 3-phosphate dehydrogenase (GAPDH; #4352339E). Data were obtained from three independent experiments and are

presented as a fold change relative to the GAPDH level of the sample.

## 2.11. Human hair organ elongation

The hair shaft was cut and cultured in growth medium under anoxic conditions with PFOB-NEs. The elongated length of the hair shaft was measured and the cut edge of the hair shaft was observed using microscopic imaging (SZX16; Olympus, Tokyo, Japan) for one week.

## 2.12. Statistical analysis

The statistical significance was evaluated using the Student's *t* test and one-way analysis of variance, and were used for the hair elongation experiment.

# 3. Results

## 3.1. Physicochemical properties of PFOB-NEs

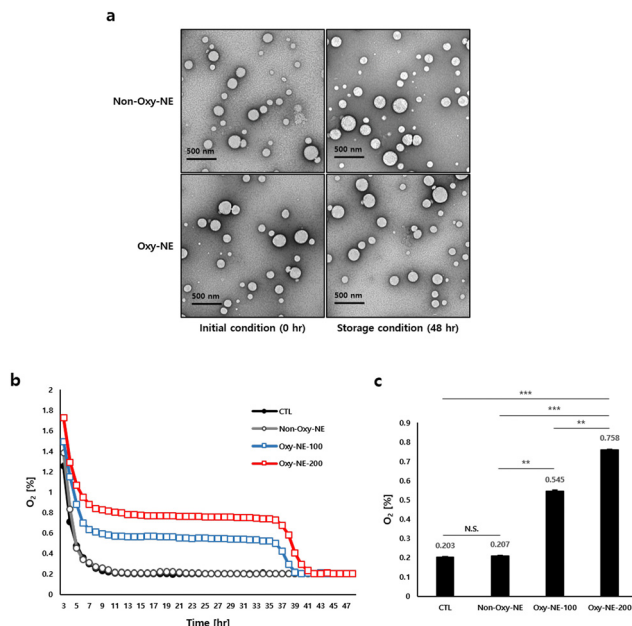
Two types of NEs with PFOB were fabricated using emulsification with and without O<sub>2</sub> purging (Oxy-NE and non-Oxy-NE, respectively). As shown in Table 1, each NE is characterized to evaluate its physicochemical properties. The particle diameters of non-Oxy-NE and Oxy-NE are  $191.50 \pm 2.08$  nm and  $192.36 \pm 0.82$  nm, the PDIs are  $0.19 \pm 0.01$  and  $0.21 \pm 0.01$ , and the corresponding zeta potentials are  $-9.59 \pm 0.92$  mV and  $-9.16 \pm 0.49$  mV, respectively. The PDI values of both emulsions confirmed that the emulsions were well prepared and homogeneous with the analyzed particle diameter. Depending on O<sub>2</sub> encapsulation, the NEs exhibit no marked changes in diameter distribution or zeta potential. After 48 h of storage at 37 °C, the diameter, PDI and zeta potential were further analyzed (Table 1, 4th line). The particle diameter of NEs increases slightly upon exposure to physiological temperature, regardless of O<sub>2</sub> encapsulation. The particle distribution did not change significantly, indicating that the particles were still homogeneous in size. In addition, the zeta potentials are not significantly affected by O<sub>2</sub> encapsulation or temperature in any given experiment. Transmission electron microscopy (TEM) images of the NEs were obtained to confirm their appearance and structural changes. As shown in Fig. 1a, all the fabricated NEs are spherical, consistent with the particle diameter ( $\sim 200$  nm). All the NEs maintained their physical

Table 1 Storage stabilities of PFOB-NEs based on their physical properties at 37 °C

Parameter	Formulation	Time (h)	
		Initial condition (0 h)	Storage condition (after 48 h)
Particle diameter (nm)	<sup>a</sup> Non-Oxy-NE	$192.36 \pm 0.82$	$218.23 \pm 5.68$
	<sup>b</sup> Oxy-NE	$191.50 \pm 2.08$	$214.30 \pm 6.49$
Polydispersity index (PDI)	<sup>a</sup> Non-Oxy-NE	$0.19 \pm 0.01$	$0.22 \pm 0.01$
	<sup>b</sup> Oxy-NE	$0.21 \pm 0.01$	$0.20 \pm 0.02$
Zeta potential (mV)	<sup>a</sup> Non-Oxy-NE	$-7.28 \pm 1.53$	$-11.39 \pm 1.36$
	<sup>b</sup> Oxy-NE	$-9.59 \pm 0.92$	$-8.94 \pm 0.73$

<sup>a</sup> Non-Oxy-NE: PFOB-NE without O<sub>2</sub>. <sup>b</sup> Oxy-NE: PFOB-NE with O<sub>2</sub>.





**Fig. 1 Concentration of O<sub>2</sub> in a liquid environment.** (a) TEM image of NE with or without O<sub>2</sub>. (b) Each concentration of O<sub>2</sub> in cell culture media was monitored every 2 h for 2 d. (c) Each concentration of O<sub>2</sub> was determined 24 h after treatment using PFOB-NE with or without O<sub>2</sub>. All O<sub>2</sub> concentration data were recorded in triplicate ( $p < 0.05$ ) and were statistically analyzed by one-way analysis of variance: \*\* $p < 0.01$ , \*\*\* $p < 0.001$ . In addition, each abbreviation was presented as follows: not significant (N.S.) and control (CTL).

properties without marked changes for two days at the physiological temperature, implying that the NEs were stable during the subsequent experiments.

### 3.2. Effect of Oxy-NE on dissolved O<sub>2</sub> concentration

Prior to the main experiments, the viability of hDPCs in PFOB-NE with or without O<sub>2</sub> purging was confirmed, indicating that PFOB-NE is a safe material (Fig. S1a, ESI†). According to the results obtained from measuring the oxygen concentrations of the PFOB-NE groups under the given conditions, it was observed that the Oxy-NE group emitted higher levels of O<sub>2</sub> compared to the control and Non-Oxy-NE groups and maintained these elevated levels for 36 h (Fig. 1b). The PFOB-NEs containing O<sub>2</sub>, particularly the Oxy-NE-200 (treated with 200  $\mu$ g mL<sup>-1</sup> PFOB-NE), released O<sub>2</sub> in the cell culture medium approximately at a level of 0.8%, which was higher than the level of approximately 0.55% observed with the treatment of 100  $\mu$ g mL<sup>-1</sup> PFOB-NE (Oxy-NE-100) after 24 h. This corresponded to the 2.68-fold higher levels for Oxy-NE-100 and 3.73-fold higher levels for Oxy-NE-200 compared to the Non-Oxy-NE group (Fig. 1c). In our preliminary study, the Oxy-NE-200 group also showed no statistical difference from the Oxy-NE-500 group, suggesting that Oxy-NE-200 sufficiently reached a steady state under physiological conditions. In this aspect, Oxy-NE-100 and 200 were focused on additional experiments (Fig. S1b, ESI†). In summary, Oxy-NEs demonstrated the ability to increase O<sub>2</sub> concentrations in the physiological microenvironment where cells existed and also sustained O<sub>2</sub> levels to a certain extent.

The physiological conditions were classified into three categories depending on the O<sub>2</sub> concentration, *viz.* normoxia, hypoxia, and anoxia. To establish the appropriate conditions for cell culture, hDPC were cultured for 24 h in normoxia (22% O<sub>2</sub>), hypoxia (2% O<sub>2</sub>), or anoxia (0.2% O<sub>2</sub>) incubators, and the O<sub>2</sub> concentrations were detected under the given conditions. The concentration of dissolved O<sub>2</sub> in the medium was found to be lower than the level of ambient air within the 37 °C incubator, under normoxic and hypoxic conditions. Particularly, under normoxic conditions, the medium containing cells had an oxygen concentration of 13.37 ± 0.07%, whereas under hypoxic conditions, it was 1.34 ± 0.01% O<sub>2</sub> in the presence of cells. However, upon examining the anoxic conditions, both the ambient air and the medium containing cells in an incubator maintained nearly identical levels of O<sub>2</sub> concentration (Fig. S1c, ESI†). Therefore, we propose that the anoxic conditions, which maintain a uniform oxygen concentration under both the incubator atmosphere and the cell culture medium, are suitable for subsequent experiments.

### 3.3. Effect of Oxy-NEs on hDPC growth under anoxic conditions

Based on the observations of the morphological and quantitative changes in hDPCs under conditions of decreased oxygen concentration in the medium without serum, it was found that despite showing relatively unhealthy morphological changes in all groups (Fig. 2a, 1st row), the absence of serum under the given experimental conditions did not have a significant impact on cell viability compared to the control groups (Fig. 2b). However, in the case of cell culture with serum included in the medium, we observed higher cell proliferation under hypoxic conditions compared to normal oxygen levels and also confirmed that anoxia maintained an intermediate level between normal oxygen and hypoxic conditions (Fig. 2a, 2nd row). Under anoxic conditions, hDPCs had a significant impact on cell growth and proliferation when treated with Oxy-NEs. Upon closer examination, under conditions of nutrient deficiency, such as the absence of serum, Oxy-NE-200 showed a greater effect in maintaining cell morphology compared to Oxy-NE-100 (Fig. 2a, 5th in 1st row); however, in the presence of serum, no distinct morphological differences, including cell numbers, were observed between the groups treated with Oxy-NE-100 and Oxy-NE-200 (Fig. 2a, 2nd row). In the absence of serum in the medium, hDPCs were found to grow and proliferate due to oxygen supply provided by Oxy-NEs (Fig. 2a, 1st row), and these effects were similar to the results observed in the presence of 10% serum (Fig. 2a, 2nd row). To quantitatively compare the results, the number of hDPCs grown per cell type is presented in Fig. 2b.

### 3.4. Oxy-NE regulates lactate accumulation and lactate dehydrogenase activity in hDPC under anoxic conditions

To assess and simulate the anoxic state of the human scalp in *in vitro* experiments, we compared the intracellular changes in hDPCs cultured under anoxic and normoxic conditions. Fig. 3a shows that the total lactate production level was approximately



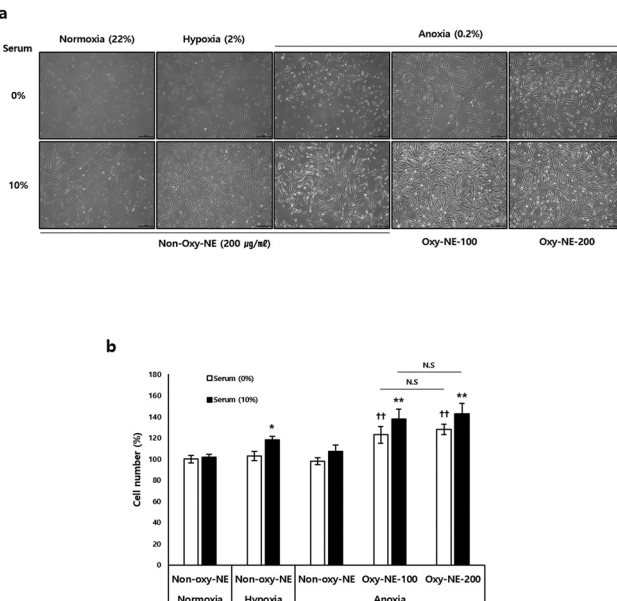


**Fig. 2 Physiological effects of Oxy-NEs on hDPCs.** (a) Morphological changes of hDPCs ( $n = 3$ ) observed when cells were co-cultured with PFOB-NEs with or without  $O_2$  under normoxic, hypoxic, or anoxic conditions (scale bar = 200  $\mu$ m). (b) Total cell number was counted under each condition. All experimental data are presented as mean  $\pm$  SD ( $n = 3$ ). All analyses were performed using unpaired Student's *t*-test and the statistical significances are presented as follows; \* $p < 0.05$ , \*\* $p < 0.01$ , and \*\*\* $p < 0.001$ , compared with non-Oxy-NE with 10% serum in normoxia, and †† $p < 0.01$ , compared with non-Oxy-NE without serum under normoxic conditions.

three times higher under anoxic conditions compared to normoxic conditions. Lactate dehydrogenase (LDH) activity was significantly lower under anoxic conditions than under normoxic conditions (Fig. 3b); however, upon treatment with Oxy-NEs for two days, LDH activity gradually increased and showed statistical significance (Fig. 3b, white bar). To investigate the underlying mechanisms of lactate production and LDH activity at the cellular level, we analyzed the expression of LDH isoforms (LDHA and LDHB) using real-time quantitative polymerase chain reaction (RT-qPCR) (Fig. S2, ESI†). The results showed that Oxy-NE treatment under anoxic conditions regulated the expression patterns of both LDHA and LDHB. Despite a concentration-dependent decrease in LDHA and LDHB expressions in response to increasing levels of Oxy-NE, the relative expression ratio between the two genes differed. As depicted in Fig. 3c, these findings indicate a higher expression level of LDHB compared to LDHA. In summary, Oxy-NEs reduced lactate production *via* suppressing LDH production and activity and also modulated oxygen concentrations in the anoxic microenvironment, ultimately influencing hDPC growth and proliferation. These findings suggest that changes in oxygen concentrations mediated by Oxy-NEs have implications beyond LDH activity and lactate accumulation and underscore the significance of oxygen supply under conditions characterized by oxygen and nutrient deprivation, such as the alopecia environment.

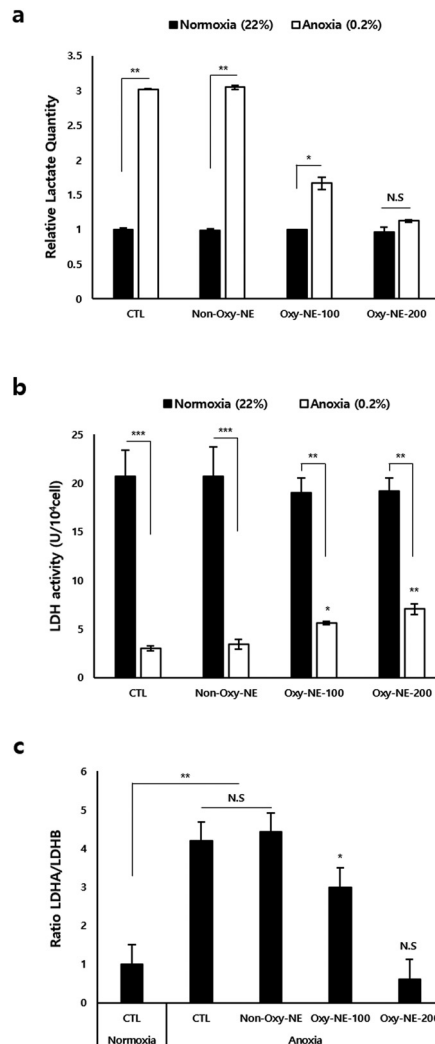


**Fig. 3 Lactate accumulation and LDH activity in hDPCs depending on  $O_2$  supply under normoxic or anoxic conditions.** (a) Each level of lactate accumulation and (b) lactate dehydrogenase (LDH) activity was measured via enzyme-linked immunosorbent assay (ELISA). (c) Comparative analysis of LDHA and LDHB expression levels in cultured hDPC under normal or hypoxic conditions. All analyses were performed using unpaired Student's *t*-test: \* $p < 0.05$ , \*\* $p < 0.01$ , and \*\*\* $p < 0.001$ , compared with the control group under normoxic conditions.

### 3.5. Oxy-NEs regulate the expression of mRNA associated with the $O_2$ reaction

A low oxygen concentration affects the microenvironment of the hair follicles *via* molecular switching of the intracellular signal transduction pathways.<sup>21,35</sup> A key component governing these pathways is the hypoxia-inducible factor (HIF), which is a transcription factor responding to decreased oxygen availability.<sup>36</sup> As shown in Fig. 4a, HIFs were downregulated under anoxic conditions. Particularly, HIF1 $\alpha$  exhibited more than a two-fold decrease in expression compared to HIF1 $\beta$ ; however, treatment with Oxy-NEs, which provided oxygen in a concentration-dependent manner, restored the expression of HIF1 $\beta$  to levels similar to that of the normoxic control group. On treatment with Oxy-NE-200, HIF1 $\alpha$  exhibited an increase of more than two-fold compared to the



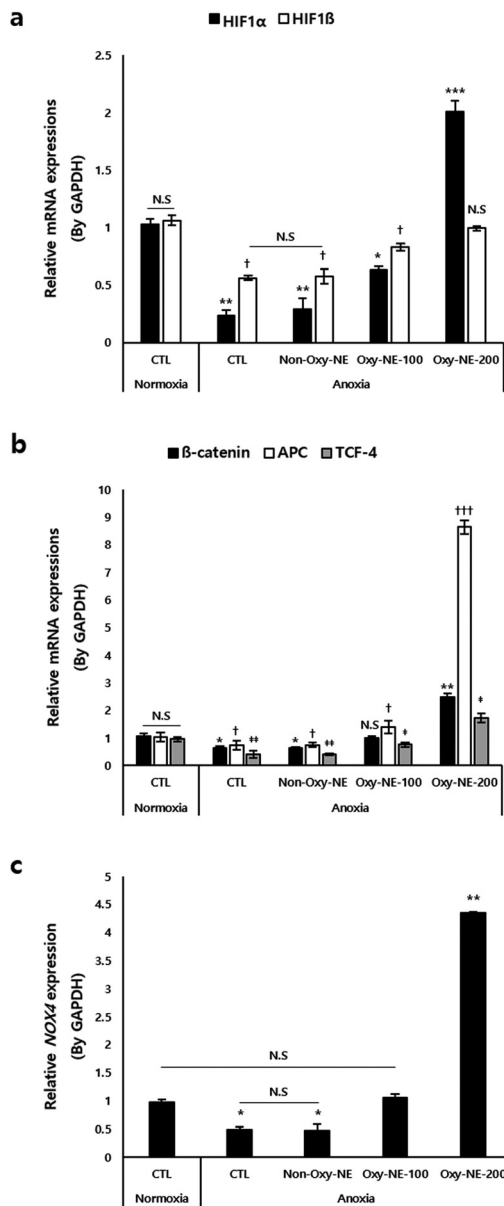


**Fig. 4** Cellular and molecular changes of mRNA levels associated with  $O_2$  depending on  $O_2$  supply. (a) Hypoxia inducing factors HIF $\alpha$  and HIF $\beta$  were quantitatively analyzed. (b)  $\beta$ -catenin, APC, T-cell factor 4 (TCF-4), and (c) NADPH oxidase 4 (NOX4) were investigated using real-time quantitative polymeric chain reaction. Data were expressed as mean  $\pm$  SD ( $n = 3$ ): \* $^{\dagger}$ \*\* $p < 0.05$ , \*\* $^{\ddagger}$ \*\* $p < 0.01$ , and \*\*\* $^{\dagger\dagger}$ \*\*\* $p < 0.001$  compared with each gene in the control group under normoxic conditions.

control group under normoxic conditions (Fig. 4a, black bar), whereas the gene expression levels of HIF1 $\beta$  were restored to that of normoxic conditions (Fig. 4a, white bar). These results indicate that, among the two HIF isotypes, HIF1 $\alpha$  exhibits greater sensitivity and responsiveness to changes in oxygen concentration, highlighting its role in oxygen level fluctuations.

Next, we examined the gene expression of  $\beta$ -catenin, adenomatous polyposis coli (APC), and T-cell factor 4 (TCF-4), which have been reported to be associated with the oxygen concentration and involved in downstream signaling mechanisms of

the Wnt/ $\beta$ -catenin pathway.<sup>37,38</sup> In Fig. 4b, the relevant genes showed decreased expression under anoxic conditions compared to that of the normoxic control group, demonstrating a concentration-dependent increase in expression upon treatment with Oxy-NEs. Treatment with Oxy-NE-200 under anoxic conditions increased the expression of these genes and also significantly elevated them, particularly with APC and TCF-4 showing an approximate two-fold and nine-fold increase compared to the control group, respectively (Fig. 4b, black and white bar).

Previous studies have reported that hDPCs exposed to low oxygen conditions activated NADPH oxidase 4 (NOX4), which regulated reactive oxygen species (ROS) and related oxidative signaling mechanisms.<sup>22,39</sup> Therefore, we investigated the expression changes of the NOX4 gene under anoxic conditions induced by Oxy-NE. Similar to the expression patterns observed in the previously examined genes, we observed a decrease in NOX4 gene expression under anoxic conditions. Treatment with Oxy-NE-100 resulted in expression levels similar to those of the control group, whereas Oxy-NE-200 treatment led to a significant increase in expression, exceeding four-fold (Fig. 4c).

In summary, even well-known factors responsive to oxygen levels were observed to be significantly suppressed under anoxic conditions; however, despite the treatment of less than 48 h, the oxygen supply mediated by Oxy-NEs effectively regulated the overall oxygen-responsive genes, including previously validated genes such as HIF1 $\beta$  and NOX4, suggesting the potential of inducing micro-environmental changes to promote hair growth *via* sensitively modulating the expression of related genes.

### 3.6. Effect of Oxy-NEs on elongation of human hair follicle organs

Human hair follicle organs were obtained and cultured under anoxic conditions for seven days, and morphological changes were observed and the hair shaft length was measured (Fig. 5 and Fig. S3, ESI<sup>†</sup>). According to the tracking results, no discernible morphological differences in human hair follicle organs between the untreated and Non-Oxy-NE-treated groups (Fig. 5a, left and center panels) and no quantitative changes in the hair shaft length during the culture period were observed (Fig. 5b). However, when with Oxy-NE-200 under the conditions, significant morphological growth was observed in the hair shaft length compared to the untreated or non-Oxy-NE-treated control group (Fig. 5a, right), and the elongation increased by approximately four-fold compared to the control group (Fig. 5b). The results indicate that anoxic conditions play a crucial role in hair growth inhibition and also emphasize the importance of regulating oxygen concentration within the biological tissue for hair regeneration. Oxygen supply using Oxy-NEs under conditions such as anoxia associated with hair loss, presents a novel strategic solution that can provide a favorable environment for human hair regeneration.

## 4. Discussion

Hair follicles undergo hair growth cycles, such as anagen, catagen, and telogen states, which are affected by vascular



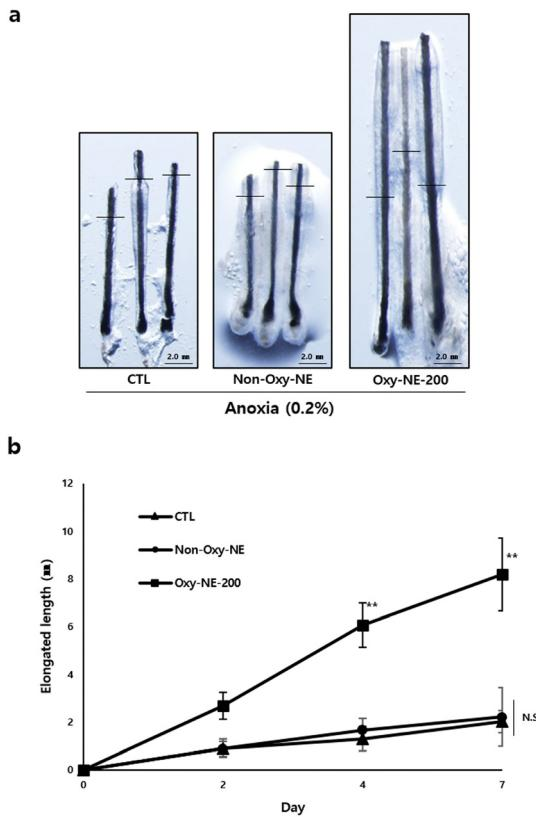


**Fig. 5 Elongation of human hair follicles after treatment with Oxy-NEs under anoxic conditions.** Isolated human scalp hair follicles were cultured for 7 d under anoxic conditions with or without O<sub>2</sub>. (a) Photograph of increased hair length on day 7. Original magnification: 40×; scale bar: 2.0 mm. (b) Data were presented as the elongated length of hair follicles without treatment, treated with non-Oxy-NE and Oxy-NE-200. Data are reported as mean ± S.E and analyzed by one-way analysis of variance. \*p < 0.05, \*\*p < 0.01 was used to compare to CTL at day 0.

supports;<sup>1–3</sup> blood vessels are important for hair growth as they eliminate wastes and supply nutrients and O<sub>2</sub>.<sup>9,10,16–20</sup> Recent studies have revealed that VEGF-induced angiogenesis promotes perifollicular vascularization, increases hair growth rate, and increases hair follicle number.<sup>18,26</sup> To provide a favorable environment, minoxidil, an FDA-approved drug, has been commercially used as an indirect inducer of angiogenesis; this promotes the conservation of vascularization for hair dermal papillae. To date, minoxidil and inhibitors of dihydrotestosterone (e.g., finasteride) are the only FDA-approved medical treatments in practice.<sup>27,40,41</sup> Minoxidil improves vascular compliance *via* relaxing the arteries and increasing their diameter, leading to improved hair growth. Overall, blood vessels on the scalp are key to hair growth; in this study, we focused on their functions, such as O<sub>2</sub> supply, instead of the nutrient content.

Recent studies have primarily focused on regional O<sub>2</sub> concentration, which varies depending on skin location.<sup>42,43</sup> The O<sub>2</sub> concentration in the epidermis is known to range widely from 0.2 to 8% in general. O<sub>2</sub> concentration around the hair follicles in the scalp skin is considerably lower, ranging from 0.1 to 0.8%, compared to that under normoxic conditions.<sup>44</sup>

Previous studies have mentioned that hypoxic conditions during the *in vitro* culture of DPCs promote their proliferation and migration, whereas normal conditions can induce oxidative stress, including the generation of ROS.<sup>22,45</sup> Hypoxic environments seem to play a role in maintaining healthy human skin and are advantageous for the proliferation and regeneration of related cells.<sup>42</sup> Furthermore, a significant accumulation of lactate has been reported in patients with hair loss, which is believed to result from oxygen deficiency.<sup>21,23</sup> Thus, adequate oxygen supply at appropriate levels can be inferred to be essential for different bodily organs, including the skin, and it is finely regulated at levels lower than that of atmospheric oxygen. In the case of hair loss, narrowing of blood vessels during hair follicle miniaturization can impede nutrient supply to the scalp area and also pose significant challenges to scalp homeostasis, which is finely regulated by minute amounts of oxygen. Consequently, the anoxic conditions thus reached play a role in the complex mechanisms associated with lactate accumulation and/or inhibition of LDH activity in hDPCs within the scalp, suggesting that alopecia is inevitably accelerated. Hence, we focused on the concomitant effects related to lactate accumulation and/or LDH activity on hDPCs under anoxic conditions.

Based on these findings, our hypothesis proposes that sustained and continuous oxygen supply to the scalp is crucial for the survival and regrowth of hDPCs, particularly during growth retardation or stagnation due to oxygen deficiency. This hypothesis indicates the potential of oxygen supply to improve micro-environmental changes associated with hair loss. We first investigated whether the growth induction of hDPCs was retarded and inhibited under conditions of severely reduced oxygen (0.2% O<sub>2</sub>) to mimic reduced vascular compliance. Subsequently, we increased the oxygen concentration through co-incubation with two limited types of Oxy-NEs: a lower zone (improved to 0.54 ± 0.005% O<sub>2</sub> concentration using Oxy-NE-100) and an upper zone (improved to 0.76 ± 0.004% O<sub>2</sub> concentration using Oxy-NE-200) (Fig. 1). These results confirmed that hDPCs exhibited robust growth without any morphological changes when co-cultured with Oxy-NEs in both zones, even under severely reduced oxygen conditions as low as 0.5–0.8%, which is lower than the 2% hypoxic condition (Fig. 2a and b). Moreover, the ability of hDPCs to proliferate in the absence of serum, along with the increased cell number in the presence of Oxy-NEs, suggested that oxygen takes precedence over nutrients in supporting hDPC growth. In conclusion, this study provides compelling evidence for the essential roles of oxygen and nutrients in hDPC survival and growth while emphasizing the synergistic effect of Oxy-NEs and serum. Particularly, oxygen is of significant importance and comparable to serum under anoxic conditions. Maintaining an optimal oxygen concentration is crucial for supporting hDPC survival, growth, and proliferation during hair miniaturization with restricted nutrient supply.

To clarify the cellular and molecular changes in O<sub>2</sub> concentrations, we first focused on both lactate accumulation and LDH activity as intracellular O<sub>2</sub> is closely associated with



biological systems. As shown in Fig. 3, hDPCs under anoxic conditions exhibited a drastic decrease in LDH activity, which regulates the total amount of lactate accumulation and production compared to those under normoxic conditions. These *in vitro* data strongly suggest that extreme hypoxic conditions can lead to lactate accumulation in the lesion of alopecia patients' due to oxygen deprivation. Oxygen supply through Oxy-NEs under anoxic conditions demonstrated nearly restored lactate accumulation to normal levels; however, LDH activity revealed a limitation in recovery, remaining at less than half of its normal level (Fig. 3b, white bar). The diminished recovery of LDH activity compared to the reduction in lactate accumulation due to oxygen supply may be attributed to the response of the biological defense system striving for efficient adaptation in oxygen-deficient environments, which warrants further investigation.

To gain a better understanding of the cellular and molecular mechanisms arising from anoxic conditions and subsequent subtle changes in oxygen concentration considered under artificial *in vitro* hair loss conditions, we examined the expression changes of genes associated with oxygen responsiveness (Fig. 4). We first focused on HIF1 (Fig. 4a), including the  $\alpha$ - and  $\beta$ -types, which are the main heterodimeric transcription factors regulating the cellular adaptive response to hypoxia.<sup>34</sup> When examining the expression patterns of HIFs, the responsiveness varied depending on the genetic isotype when artificially controlling the oxygen concentration using Oxy-NEs. Particularly, the results revealed that HIF1 $\alpha$ , which is well-known for its preferential response under hypoxic conditions, responded more sensitively to changes in the oxygen concentration compared to HIF1 $\beta$ . These findings may not be limited to the case of HIFs alone. Under anoxic conditions, treatment with Oxy-NE-200 led to a significant and rapid increase in the expression of APC, a gene associated with Wnt/ $\beta$ -catenin signaling, which was even more pronounced than the response of  $\beta$ -catenin or TCF-4, exceeding nine-fold compared to normoxic conditions (Fig. 4b). Lastly, upon reaching anoxic conditions, NOX4, a key regulatory factor known to be involved in the control of Wnt signaling, survival, and growth of hDPCs during *in vitro* cell culture,<sup>22,37</sup> showed a drastic decrease in expression compared to the control group; however, it exhibited an approximate five-fold higher expression when oxygen supply was provided (Fig. 4c). Therefore, genes that respond sensitively to oxygen supply under extreme survival conditions, such as anoxia, may likely be essential for maintaining cell viability and homeostasis, which necessitates further research to explore this relationship in detail.

According to the final validation using the human hair follicle organs, the absence of complete growth inhibition in the untreated and non-Oxy-NE control groups can be inferred as a result of the inability to achieve complete oxygen deprivation during the Oxy-NE treatment process and the mild responsiveness of the organ to temporary normoxic conditions (Fig. 5a, left and center). However, under the same conditions, the supply and maintenance of oxygen at a concentration level of 0.8% *via* Oxy-NE-200 significantly contributed to hair growth

(Fig. 5a, right panel and Fig. 5b). This can be inferred due to the appropriate organ survival range maintained at oxygen levels of 0.2–0.8%, which further enhanced the observed effects. Although validation using animal experiments or application to actual human scalps may provide clearer possibilities, the absence of a limited experimental model solely focused on oxygen supply control, hindered the establishment of preclinical or clinical-level validation. These clinical limitations can be sufficiently overcome by further research in this field. Ultimately, the results obtained through this study indicate the enhancement of hair growth using oxygen delivery systems, positioning it as a promising next-generation strategic technology to combat hair loss.

## 5. Conclusions

Our findings demonstrate that continuous oxygen supply using Oxy-NEs under conditions such as anoxia, resembling hair loss conditions, regulates the accumulation of lactate resulting from oxygen deprivation and also influences the expression of relevant genes for hair growth, ultimately promoting the growth of hDPCs. The utilization of Oxy-NEs aims to create a favorable environment for hair regeneration and has proven to be effective in controlling local oxygen concentrations. Additionally, its uniform nanosize properties sufficiently propose the potential for strategic application through the human scalp.

## Author contributions

P. J. P. and S. T. K. conceived, designed, and performed experiments. H. M., B. S. P. and J. P. J. constructed PFC nanomaterials. P. J. P., S. T. K., and J. P. J. analyzed the data and wrote the manuscript. All authors contributed to the general discussion and have read and agreed to the published version of the manuscript.

## Conflicts of interest

There are no conflicts to declare.

## References

- 1 O. Veraitch, Y. Mabuchi, Y. Matsuzaki, T. Sasaki, H. Okuno, A. Tsukashima, M. Amagai, H. Okano and M. Ohyama, Induction of hair follicle dermal papilla cell properties in human induced pluripotent stem cell-derived multipotent LNGFR(+)THY-1(+) mesenchymal cells, *Sci. Rep.*, 2017, **7**, 42777.
- 2 T. G. Phillips, W. P. Slomiany and I. I. R. Allison, Hair Loss: Common Causes and Treatment, *Am. Fam. Physician*, 2017, **96**, 371–378.
- 3 L. C. Sperling, Hair and Systematic Disease, *Dermatol. Clin.*, 2001, **19**, 711–726.
- 4 R. L. Lin, L. Garibyan, A. B. Kimball and L. A. Drake, Systemic Causes of Hair Loss, *Ann. Med.*, 2016, **48**, 393–402.

5 E. L. Guo and R. Katta, Diet and Hair Loss: Effects of Nutrient Deficiency and Supplement Use, *Dermatol. Pract. Concept.*, 2017, **7**, 1–10.

6 S. C. Chueh, S. J. Lin, C. C. Chen, M. Lei, L. M. Wang, R. Widelitz, M. W. Hughes, T. X. Jiang and C. M. Chuong, Therapeutic Strategy for Hair Regeneration: Hair Cycle Activation, Niche Environment Modulation, Wound-Induced Follicle Neogenesis and Stem Cell Engineering, *Expert Opin. Biol. Ther.*, 2013, **13**, 377–391.

7 T. Mubki, L. Rudnicka, M. Olszewska and J. Shapiro, Evaluation and Diagnosis of the Hair Loss Patient: Part I. History and Clinical Examination, *J. Am. Acad. Dermatol.*, 2014, **71**, 415.e1–e15.

8 N. Hunt and S. McHale, The Psychological Impact of Alopecia, *BMJ*, 2005, **331**, 951–953.

9 Y. Hellsten and B. Hoier, Capillary Growth in Human Skeletal Muscle: Physiological Factors and the Balance Between Pro-Angiogenic and Angiostatic Factors, *Biochem. Soc. Trans.*, 2014, **42**, 1616–1622.

10 T. Rademakers, J. M. Horvath, C. A. van Blitterswijk and V. L. S. LaPointe, Oxygen and Nutrient Delivery in Tissue Engineering: Approaches to Graft Vascularization, *J. Tissue Eng. Regen. Med.*, 2019, **13**, 1815–1829.

11 A. M. Finner, Nutrition and Hair: Deficiencies and Supplements, *Dermatol. Clin.*, 2013, **31**, 167–172.

12 R. M. Trüeb, Serum Biotin Levels in Women Complaining of Hair Loss, *Int. J. Trichology*, 2016, **8**, 73–77, DOI: [10.4103/0974-7753.188040](https://doi.org/10.4103/0974-7753.188040).

13 C. Le Floc'h, A. Cheniti, S. Connétable, N. Piccardi, C. Vincenzi and A. Tosti, Effect of a Nutritional Supplement on Hair Loss in Women, *J. Cosmet. Dermatol.*, 2015, **14**, 76–82.

14 H. M. Almohanna, A. A. Ahmed, J. P. Tsatalis and A. Tosti, The Role of Vitamins and Minerals in Hair Loss: A Review, *Dermatol. Ther.*, 2019, **9**, 51–70.

15 J. M. Thompson, M. A. Mirza, M. K. Park, A. A. Qureshi and E. Cho, The Role of Micronutrients in Alopecia Areata: A Review, *Am. J. Clin. Dermatol.*, 2017, **18**, 663–679.

16 N. Zerbinati, S. Sommatis, C. Maccario, M. C. Capillo, S. D. Di Francesco, R. Rauso, M. Protasoni, E. D'Este, D. D. Gasperina and R. Mocchi, *In Vitro* Hair Growth Promoting Effect of a Noncrosslinked Hyaluronic Acid in Human Dermal Papilla Cells, *BioMed Res. Int.*, 2021, **2021**, 5598110.

17 H. Kato, K. Kinoshita, N. Saito, K. Kanayama, M. Mori, N. Asahi, A. Sunaga, K. Yoshizato, S. Itami and K. Yoshimura, The Effects of Ischemia and Hyperoxigenation on Hair Growth and Cycle, *Organogenesis*, 2020, **16**, 83–94.

18 T. Kageyama, Y. S. Chun and J. Fukuda, Hair Follicle Germs Containing Vascular Endothelial Cells for Hair Regenerative Medicine, *Sci. Rep.*, 2021, **11**, 624.

19 C. M. Snyder and N. S. Chandel, Mitochondrial Regulation of Cell Survival and Death During Low-Oxygen Conditions, *Redox Signal.*, 2009, **11**, 2673.

20 M. Semalty, A. Semalty, G. P. Joshi and M. S. M. Rawat, Hair Growth and Rejuvenation: An Overview, *J. Dermatol. Treat.*, 2011, **22**, 123–132.

21 K. N. Li, P. Jain, C. H. He, F. C. Eun, S. J. Kang and T. Tumbar, Skin Vasculature and Hair Follicle Cross-Talking Associated with Stem Cell Activation and Tissue Homeostasis, *eLife*, 2019, **8**, e45977.

22 M. Zheng, Y. Jang, N. Choi, D. Y. Kim, T. W. Han, J. H. Yeo, J. Lee and J. H. Sung, Hypoxia Improves Hair Inductivity of Dermal Papilla Cells via Nuclear NADPH Oxidase 4-Mediated Reactive Oxygen Species Generation, *Br. J. Dermatol.*, 2019, **181**, 523–534, DOI: [10.1111/bjd.17706](https://doi.org/10.1111/bjd.17706).

23 A. Flores, J. Schell, A. S. Krall, D. Jelinek, M. Miranda, M. Grigorian, D. Braas, A. C. White, J. L. Zhou, N. A. Graham, T. Graeber, P. Seth, D. Evseenko, H. A. Coller, J. Rutter, H. R. Christofk and W. E. Lowry, Lactate Dehydrogenase Activity Drives Hair Follicle Stem Cell Activation, *Nat. Cell Biol.*, 2017, **19**, 1017–1026.

24 J. Ye, X. Tang, Y. Long, Z. Chu, Q. Zhou and B. Lin, The Effect of Hypoxia on the Proliferation Capacity of Dermal Papilla Cell by Regulating Lactate Dehydrogenase, *Cosmet. Dermatol.*, 2021, **20**, 684–690.

25 K. Yano, L. F. Brown and M. Detmar, Control of Hair Growth and Follicle Size by VEGF-Mediated Angiogenesis, *J. Clin. Invest.*, 2001, **107**, 409–417.

26 S. Lachgar, M. Charveron, Y. Gall and J. L. Bonafe, Minoxidil Upregulates the Expression of Vascular Endothelial Growth Factor in Human Hair Dermal Papilla Cells, *Br. J. Dermatol.*, 1998, **138**, 407–411.

27 N. Choi, S. Shin, S. U. Song and J. Sung, Minoxidil Promotes Hair Growth through Stimulation of Growth Factor Release from Adipose-Derived Stem Cells, *Int. J. Mol. Sci.*, 2018, **19**, 691, DOI: [10.3390/ijms19030691](https://doi.org/10.3390/ijms19030691).

28 M. P. Krafft and J. G. Riess, Therapeutic Oxygen Delivery by Perfluorocarbon-Based Colloids, *Adv. Colloid Interface Sci.*, 2021, **294**, 102407.

29 J. G. Riess, Understanding the Fundamentals of Perfluorocarbons and Perfluorocarbon Emulsions Relevant to *In Vivo* Oxygen Delivery, *Artif. Cells, Blood Substitutes, Biotechnol.*, 2005, **33**, 47–63.

30 C. I. Castro and J. C. Briceno, Perfluorocarbon-Based Oxygen Carriers: Review of Products and Trials, *Artif. Organs*, 2010, **34**, 622–634.

31 J. Jägers, A. Wrobeln and K. B. Ferenz, Perfluorocarbon-Based Oxygen Carriers: From Physics to Physiology, *Eur. J. Physiol.*, 2021, **473**, 139–150.

32 M. Nieuwoudt, G. H. C. Engelbrecht, L. Sentle, R. Auer, D. Kahn and S. W. van der Merwe, Non-toxicity of IV Injected Perfluorocarbon Oxygen Carrier in an Animal Model of Liver Regeneration Following Surgical Injury, *Artif. Cells, Blood Substitutes, Biotechnol.*, 2009, **37**, 117–124.

33 E. G. Schutt, D. H. Klein, R. M. Mattrey and J. G. Riess, Injectable Microbubbles as Contrast Agents for Diagnostic Ultrasound Imaging: The Key Role of Perfluorochemicals, *Angew. Chem., Int. Ed.*, 2003, **42**, 3218–3235.

34 J. P. Jee, R. Pangeni, S. K. Jha, Y. Byun and J. W. Park, Preparation and *in vivo* Evaluation of a Topical Hydrogel System Incorporating Highly Skin-Permeable Growth Factors, Quercetin, and Oxygen Carriers for Enhanced



Diabetic Wound-Healing Therapy, *Int. J. Nanomed.*, 2019, **14**, 5449–5475.

35 L. Varela-Nallar, M. Rojas-Abalos, A. C. Abbott, E. A. Moya, R. Iturriaga and N. C. Inestrosa, Chronic Hypoxia Induces the Activation of the Wnt/β-Catenin Signaling Pathway and Stimulates Hippocampal Neurogenesis in Wild-Type and APPswe-PS1ΔE9 Transgenic Mice *in vivo*, *Front. Cell. Neurosci.*, 2014, **8**, 17.

36 H. Zhang, W. Nan, X. Song, S. Wang, H. Si and G. Li, Knockdown of HIF-1 $\alpha$  Inhibits the Proliferation and Migration of Outer Root Sheath Cells Exposed to Hypoxia *in vitro*: An Involvement of Shh Pathway, *Life Sci.*, 2017, **191**, 82–89.

37 H. Jin, Z. Zou, H. Chang, Q. Shen, L. Liu and D. Xing, Photobiomodulation Therapy for Hair Regeneration: A Synergetic Activation of β-CATENIN in Hair Follicle Stem Cells by ROS and Paracrine WNTs, *Stem Cell Rep.*, 2021, **16**, 1568–1583.

38 J. Mazumdar, W. T. O'Brien, R. S. Johnson, J. C. LaManna, J. C. Chavez, P. S. Klein and M. C. Simon, O<sub>2</sub> Regulates Stem Cells through Wnt/β-Catenin Signalling, *Nat. Cell Biol.*, 2010, **12**, 1007–1013.

39 Y. Nisimoto, B. A. Diebold, D. Cosentino-Gomes and J. D. Lambeth, Nox4: A Hydrogen Peroxide-Generating Oxygen Sensor, *Biochemistry*, 2014, **53**, 5111–5120.

40 A. Adil and M. Godwin, The Effectiveness of Treatments for Androgenetic Alopecia: A Systematic Review and Meta-Analysis, *J. Am. Acad. Dermatol.*, 2017, **77**, 136–141.e5.

41 S. W. Lee, M. Juhasz, P. Mobasher, C. Ekelem and N. A. Mesinkovska, A Systematic Review of Topical Finasteride in the Treatment of Androgenetic Alopecia in Men and Women, *J. Drugs Dermatol.*, 2018, **17**, 457–463.

42 W. Wang, C. P. Winlove and C. C. Michel, Oxygen Partial Pressure in Outer Layers of Skin of Human Finger Nail Folds, *J. Physiol.*, 2003, **549**, 855–863.

43 S. M. Evans, A. E. Schrlau, A. A. Chalian, P. Zhang and C. J. Koch, Oxygen Levels in Normal and Previously Irradiated Human Skin as Assessed by EF5 Binding, *J. Invest. Dermatol.*, 2006, **126**, 2596–2606.

44 C. S. Kim, X. Ding, K. Allmeroth, L. C. Biggs, O. I. Kolenc, N. L'Hoest, C. A. Chacón-Martínez, C. Edlich-Muth, P. Giavalisco, K. P. Quinn, M. S. Denzel, S. A. Eming and S. A. Wickström, Glutamine Metabolism Controls Stem Cell Fate Reversibility and Long-Term Maintenance in the Hair Follicle, *Cell Metab.*, 2020, **32**, 629–642.e8.

45 L. Mecklenburg, D. J. Tobin, S. Müller-Röver, B. Handjiski, G. Wendt, E. M. Peters, S. Pohl, I. Moll and R. Paus, Active Hair Growth (Anagen) is Associated with Angiogenesis, *J. Invest. Dermatol.*, 2000, **114**, 909–916.

